MOLECULAR ONCOLOGY 10 (2016) 526–537

available at www.sciencedirect.com

ScienceDirect

www.elsevier.com/locate/molonc

Cripto: Expression, epigenetic regulation and potential diagnostic use in testicular germ cell tumors

Cassy M. Spiller[a], *Ad J.M. Gillis*[b], *Guillaume Burnet*[a,c], *Hans Stoop*[b], *Peter Koopman*[a], *Josephine Bowles*[a,1], *Leendert H.J. Looijenga*[b,*,1]

[a]*Division of Genomics of Development and Disease, Institute for Molecular Bioscience, The University of Queensland, Brisbane, QLD 4072, Australia*

[b]*Department of Pathology, Erasmus MC – University Medical Center, Rotterdam, 3015, The Netherlands*

[c]*Departement de Biologie, Ecole Normale Superieure de Cachan, Cachan, France*

ARTICLE INFO

Article history:
Received 18 June 2015
Received in revised form
3 November 2015
Accepted 3 November 2015
Available online 18 November 2015

Keywords:
Cripto
Testicular germ cell cancer
Methylation
Diagnostic

ABSTRACT

Type II germ cell tumors arise after puberty from a germ cell that was incorrectly programmed during fetal life. Failure of testicular germ cells to properly differentiate can lead to the formation of germ cell neoplasia *in situ* of the testis; this precursor cell invariably gives rise to germ cell cancer after puberty. The Nodal co-receptor Cripto is expressed transiently during normal germ cell development and is ectopically expressed in non-seminomas that arise from germ cell neoplasia *in situ*, suggesting that its aberrant expression may underlie germ cell dysregulation and hence germ cell cancer. Here we investigated methylation of the *Cripto* promoter in mouse germ cells and human germ cell cancer and correlated this with the level of CRIPTO protein expression. We found hypomethylation of the *CRIPTO* promoter in undifferentiated fetal germ cells, embryonal carcinoma and seminomas, but hypermethylation in differentiated fetal germ cells and the differentiated types of non-seminomas. CRIPTO protein was strongly expressed in germ cell neoplasia *in situ* along with embryonal carcinoma, yolk sac tumor and seminomas. Further, cleaved CRIPTO was detected in media from seminoma and embryonal carcinoma cell lines, suggesting that cleaved CRIPTO may provide diagnostic indication of germ cell cancer. Accordingly, CRIPTO was detectable in serum from 6/15 patients with embryonal carcinoma, 5/15 patients with seminoma, 4/5 patients with germ cell neoplasia *in situ* cells only and in 1/15 control patients. These findings suggest that CRIPTO expression may be a useful serological marker for diagnostic and/or prognostic purposes during germ cell cancer management.

Abbreviations: GCNIS, Germ cell neoplasia *In Situ*; CH, choriocarcinoma; dcp, days *post coitum*; ELISA, enzyme-linked immunosorbent assay; FACS, fluorescence activated cell sorting; GCC, germ cell cancer; NS, non-seminoma; SE, seminoma; TE, teratoma; YST, yolk sac tumor.

* *Corresponding author.*
E-mail address: l.looijenga@erasmusmc.nl (L.H.J. Looijenga).
[1] Joint senior authors.

http://dx.doi.org/10.1016/j.molonc.2015.11.003

1. Introduction

Testicular germ cell cancers (GCCs), also known as Type II germ cell tumors (Oosterhuis and Looijenga, 2005), account for ~60% of all malignancies in men aged 20–40 (Adami et al., 1994; van de Geijn et al., 2009). The cell of origin or 'cancer stem cell', germ cell neoplasia *in situ* (GCNIS, according to the newest WHO classification, 2016), previously known as carcinoma *in situ* (CIS) and intratubular germ cell neoplasia unclassified (IGCNU), is considered to be an embryonic germ cell that has failed to differentiate into a prespermatogonium during development (Skakkebaek et al., 1987). Although GCNIS may be present before birth, it does not transform into GCC until after puberty when tumor pathology is classified into seminoma (SE) and non-seminoma (NS) (Sonne et al., 2009; van de Geijn et al., 2009). SE is characterized by fetal germ cell-like expression profile, and NS comprises both highly pluripotent/undifferentiated tumors (embryonal carcinoma; EC) and differentiated tumors: yolk-sac tumor (YST); choriocarcinoma (CH); teratoma (TE) and combinations of these.

The 'fetal origins hypothesis' of GCNIS predicts developmental pathways that control fetal germ cell pluripotency/differentiation contribute to their malignant potential. We recently discovered that the TGFβ signaling molecule Nodal and its obligate receptor Cripto are expressed at a critical point during fetal XY germ cell development in mice and that Nodal/Cripto signaling is active, apparently acting to maintain pluripotency and oppose differentiation (Spiller et al., 2012). We also found that Nodal/Cripto signaling is ectopically activated in NS and we therefore hypothesize that ectopic activation of Nodal signaling, or failure to silence it, contributes to GCC formation (Spiller et al., 2013).

Nodal, a member of the TGFβ family, signals by binding to Activin receptors in the presence of the receptor Cripto (also known as teratocarcinoma derived growth factor 1; Tdgf1). Nodal signaling is absent in normal adult tissues, but is critical for patterning events during embryogenesis (Shen, 2007). Cripto is also essential during embryogenesis, and plays additional roles in stem cell self-renewal and pluripotency in human embryonic stem cells (Bianco et al., 2010; Wei et al., 2005). Its continuous activation is associated with initiation or progression of cancer in many tissues including skin, pancreas, intestine, breast, bladder and brain (Klauzinska et al., 2014). As a cell-surface receptor for Nodal, Cripto must remain tethered to the cell membrane via its glycosylphosphatidylinositol (GPI) anchor at its carboxy terminal (Watanabe et al., 2007b). Cleavage of Cripto at the GPI anchor by GPI-phospholipase D produces a shorter, biologically active form of Cripto that can promote endothelial cell migration, independent of Nodal signaling (Watanabe et al., 2007a). Detection of cleaved Cripto in serum has been identified as a promising diagnostic for breast, colon and brain cancer (Bianco et al., 2006; Pilgaard et al., 2014).

Hypomethylation of oncogenes and hypermethylation of tumor-suppressor genes are commonly seen in cancer, therefore it is possible that dysregulation of Cripto expression in GCC may reflect aberrant methylation of regulatory sequences. In this study we investigated the methylation status of the Cripto promoter during normal fetal germ cell development in mice and contrasted this to human GCC. We also assessed Cripto protein expression in GCNIS and GCC of different histologies. Lastly we used ELISA to quantitate levels of Cripto protein present in conditioned media from GCC cell lines and serum from patients with GCC.

2. Materials and methods

2.1. Mouse strains

Protocols and use of animals in these experiments were approved by the Animal Ethics Committee of the University of Queensland. Embryos were collected from timed matings of the CD1 strain and Oct4ΔPE:eGFP (OG2) strain (Szabo et al., 2002), with noon of the day on which the mating plug was observed designated 0.5 days post coitum (dpc).

2.2. Gonadal collection, germ cell isolation

Gonads without mesonephros were dissected at 11.5–17.5 dpc from CD1 embryos. At 11.5 dpc embryos were genotyped by PCR for genetic sex (McFarlane et al., 2013); later stages were sexed visually by gonad morphology. For each stage three pools of ≥4 gonads were processed for qRT-PCR. For germ cell isolation, sexed gonadal tissue was collected from Oct4Δ PE:eGFP matings. Tissue was dissociated and germ cell (GFP+) populations isolated by fluorescence-activated cell sorting (FACS) using a FACSAria Cell Sorter (BD Biosciences). For each sex and timepoint approximately 100,000 cells were collected and processed for methylation profiling.

2.3. Cell line culture and 5-azacytidine treatment

TCam-2 and JKT-1 were maintained in RPMI (Life Technologies), and NT2 and TERA-1 cells in DMEM (Life Technologies) with the addition of 10% fetal calf serum (GE Healthcare Life Sciences, HyClone Laboratories), 100 U/ml penicillin and 100 ug/ml streptomycin in a humidified 5% CO_2, 37 °C incubator. Treatment with 5-azacytidine (AG scientific) was used at a final concentration of 10 μM (Wermann et al., 2010).

2.4. Human GCC samples

Use of tissue samples for scientific reasons was approved by an institutional review board (MEC 02.981 and CCR2041) in The Netherlands and by the Human Research Ethics Committee at the University of Queensland. Samples were used according to the "Code for Proper Secondary Use of Human Tissue in The Netherlands" developed by the Dutch Federation of Medical and Scientific Societies (FMWV) (Version 2, update 2011). Tissues were collected as described (Looijenga et al., 2003) and diagnosed according to WHO standards by an experienced pathologist (J.W Oosterhuis, Erasmus MC, Rotterdam, The Netherlands). The testicular parenchyma samples investigated have been described previously (Mosselman et al., 1996) and comprised of tissue microarrays as well as single biopsies. Samples (paraffin blocks,

gDNA, RNA and serum) were extracted at Erasmus MC, Rotterdam, The Netherlands and selected to exemplify different histological subtypes.

2.5. Quantitative RT-PCR

Total RNA was extracted (RNeasy kit; Qiagen) and cDNA generated (High capacity cDNA Reverse Transcription kit; Applied Biosystems) according to manufacturers' instructions. Taqman probes (Applied Biosystems) used were: mouse (*Tbp*; Mm00446973_m1, *Cripto/Tdgf1*; Mm00783944_g1) and human (*TBP*; Hs00427621_m1, *CRIPTO/TDGF1*; Hs02339499_g1, *NODAL*; Hs00415443_m1, *LEFTY1*; Hs00764128_s1, *LEFTY2*; Hs00745761_s1, *SOX2*; Hs01053049_s1, *SOX17*; Hs00751752_s1, *GFD3*; Hs00220998, *DNMT3L*; Hs01081364_m1). Relative transcript abundance was calculated using the $2^{-\Delta CT}$ method. Error bars represent S.E.M calculated from independent biological replicates.

2.6. Methylation profiling – mouse germ cells

DNA was extracted (Qiagen, DNeasy kit) from freshly isolated germ cells and bisulfite-treated (Zymo Research, EZ DNA Methylation Kit). Between 2 and 4 ng of bisulfite-treated and untreated (control) DNA was subjected to two rounds of PCR amplification with Hot-start Taq DNA Polymerase (NEB) (conditions described in Supplementary Table 1). The first amplification of 35 cycles used flanking primers in a 25 μl reaction. Subsequently 1 μl of this reaction was subjected to a further 35 cycles using nested primers. PCR products were gel purified, cloned into pGEM-T Easy (Promega) and 10–15 clones sequenced using T7 and T3 primers at the Australian Genome Research Facility (Brisbane, Australia).

2.7. Methylation profiling – GCC cell lines and tumor samples

DNA was extracted from cell lines and tumor biopsies according to manufacturer's instructions (Qiagen, DNeasy kit). DNA was bisulfite-treated (Zymo Research, EZ DNA Methylation Kit) and 2.5 μg of bisulfite treated and untreated (control) DNA was subjected to one round of PCR amplification of 40 cycles with Zymo Taq DNA Polymerase (Zymo Research) (conditions described in Supplementary Table 1). PCR reactions were subjected to ExoSAP-IT PCR clean-up protocol (Affymetrix). For direct sequencing, 5 μl of the purified PCR product was used with the ABI Prism BigDye Terminator sequencing kit (Applied Biosciences, v1.1) with forward and reverse primers. For colony sequencing, 1 μl of the PCR product was cloned into the TOPO-TA vector (Life Technologies) and 10–15 clones sequenced using the ABI Prism BigDye Terminator sequencing kit (Applied Biosciences, v1.1) with M13 primer.

2.8. Immunohistochemistry

Paraffin sections (3 μm) of previously characterized tumors were deparaffinised and heated under pressure to 1.2 bar in 0.01 M Tris, 0.001 M EGTA, pH 9.0. Slides were blocked with Avidin and Biotin solution (Vector Laboratories) and incubated with monoclonal anti-CRIPTO antibody (1:10000; commissioned from Abmart; raised against epitope sequence FPQAFLPG) in 0.2%BSA/PBS overnight at 4 °C. Biotinylated Rabbit anti-mouse antibody (1:150; Dako E413) was incubated for 30 min at RT followed by incubation with Avidin-Biotin-HRP complex (Vector Laboratories) for 30 min and staining visualized with DAB reagents (Vector Laboratories). Slides were counterstained with haematoxylin and mounted.

2.9. Western blotting

NT2 cells were lysed in RIPA buffer and sonicated, run on a 10% SDS-PAGE gel, transferred to PVDF membrane then blocked/probed in 5% skim milk/PBS. Primary antibodies (anti-CRIPTO; Abmart 8295; 1:10000, TUBA1A; Sigma T5168; 1:1000) were incubated overnight at 4 °C and secondary antibodies (mouse-HRP; Sigma a8924; 1:2000) for 1 h at RT. Detection was performed using ECL (BioRad) and imaged using BioRad ChemiDoc.

2.10. Cripto ELISA

Human Cripto-1 DuoSet ELISA Development kit (DY145; R&D Systems) was used as per manufacturer's instructions. Cell culture media was diluted 1:5 with 0.1% BSA/PBS. Complete media diluted 1:5 in 0.1% BSA/PBS with standards was used as the control to generate the standard curve for interpolation. For serum analysis, whole serum was diluted 1:2 in 0.1% BSA/PBS and standards spiked into control serum diluted 1:2 in 0.1% BSA/PBS to generate the standard curve for interpolation. All standards and unknowns were assayed in duplicate. Optical density was determined using a microplate reader (Bio-Rad) with the 570 nm reading subtracted from the 450 nm reading. Duplicate readings for each sample were averaged and the zero standard optical density subtracted from this value. Prism software was used to generate a four-parameter logistic curve-fit and unknown values were interpolated to give the final CRIPTO concentration. For assessment of our commissioned CRIPTO antibody (Abmart) the ELISA assay was performed exactly as per manufacturer's instructions with the exception that the R&D Systems capture antibody was replaced with the Abmart CRIPTO antibody at a concentration of 5 ug/ml. Recombinant CIRPTO standard range was 0–4000 ng/ml.

3. Results

3.1. Cripto promoter methylation in mouse fetal germ cells

Because we have shown that Cripto is expressed for a short time in fetal germ cells but is ectopically expressed in GCC (Spiller et al., 2012), we wanted to investigate the mechanism by which Cripto expression is properly silenced under normal conditions using the mouse model. We began by investigating methylation of CpG dinucleotides in the promoter region, since male germ cells are known to undergo genome-wide remethylation from 13.5 to 18.5 days post coitum (dpc) in mice (La Salle et al., 2004; Western et al., 2010). Using Methyl Primer Express software (v1.0, Applied Biosystems) we

identified two regions in the mouse Cripto promoter with high CpG site-content. Region 1 is 1383 bp upstream of the transcription start site (15 CpG sites) and Region 2 spans the transcription start site (18 CpG sites) (Figure 1A).

To assess methylation specifically in germ cells, we isolated male and female (control) germ cells from Oct4ΔPE:eGFP mouse embryos (Szabo et al., 2002) using FACS at 13.5 dpc (*Cripto* is expressed in the male) and at 17.5 dpc (expression has declined in the male; Figure 1B, Supplementary Figure 1). Bisulfite-treated DNA was subjected to PCR amplification of the two CpG regions before cloning and sequence analysis. We found that XX (female) germ cells displayed increased methylation in Region 1 from 13.5 to 17.5 dpc (6%–24% average methylation) while methylation of Region 2 remained unchanged (27% both timepoints; Figure 1C). Conversely, XY (male) germ cells displayed an increase in methylation of Region 2 from 13.5 to 17.5 dpc (22%–56%), whilst CpG sites in Region 1 remained unmethylated at both timepoints (1% and 0%) (Figure 1C). These data indicate that methylation of CpG sites in Region 2 correlates with declining *Cripto* expression male germ cells.

3.2. *CRIPTO promoter methylation in human GCC*

We next investigated whether methylation of the human *CRIPTO* promoter might also correlate with levels of gene expression in the various GCC specimens, using a combination of direct- and colony-bisulfite sequencing. The human *CRIPTO* proximal promoter contains two CpG regions that contain 14 and 7 CpG sites, respectively (Figure 2A). These regions have previously been shown in the EC cell line NT2/D1 to be differentially methylated according to expression level and potential malignancy of these cells (Watanabe et al., 2010).

Gene expression of *CRIPTO* was highest in EC and YST, with low transcript expression detectable in SE, TE and CH samples (Figure 2B). By colony sequencing, CH and TE (low *CRIPTO* expression) displayed high levels of methylation (average 75% and 72%, respectively) in both regions (Figure 2C,D). Conversely, in EC, which displays high levels of *CRIPTO* expression, methylation levels were relatively low (20%; Figure 2E). In contrast, despite high expression of *CRIPTO* in YST, both regions remained moderately-to-highly methylated (67%; Figure 2F). Further, in SE, which expresses low levels of

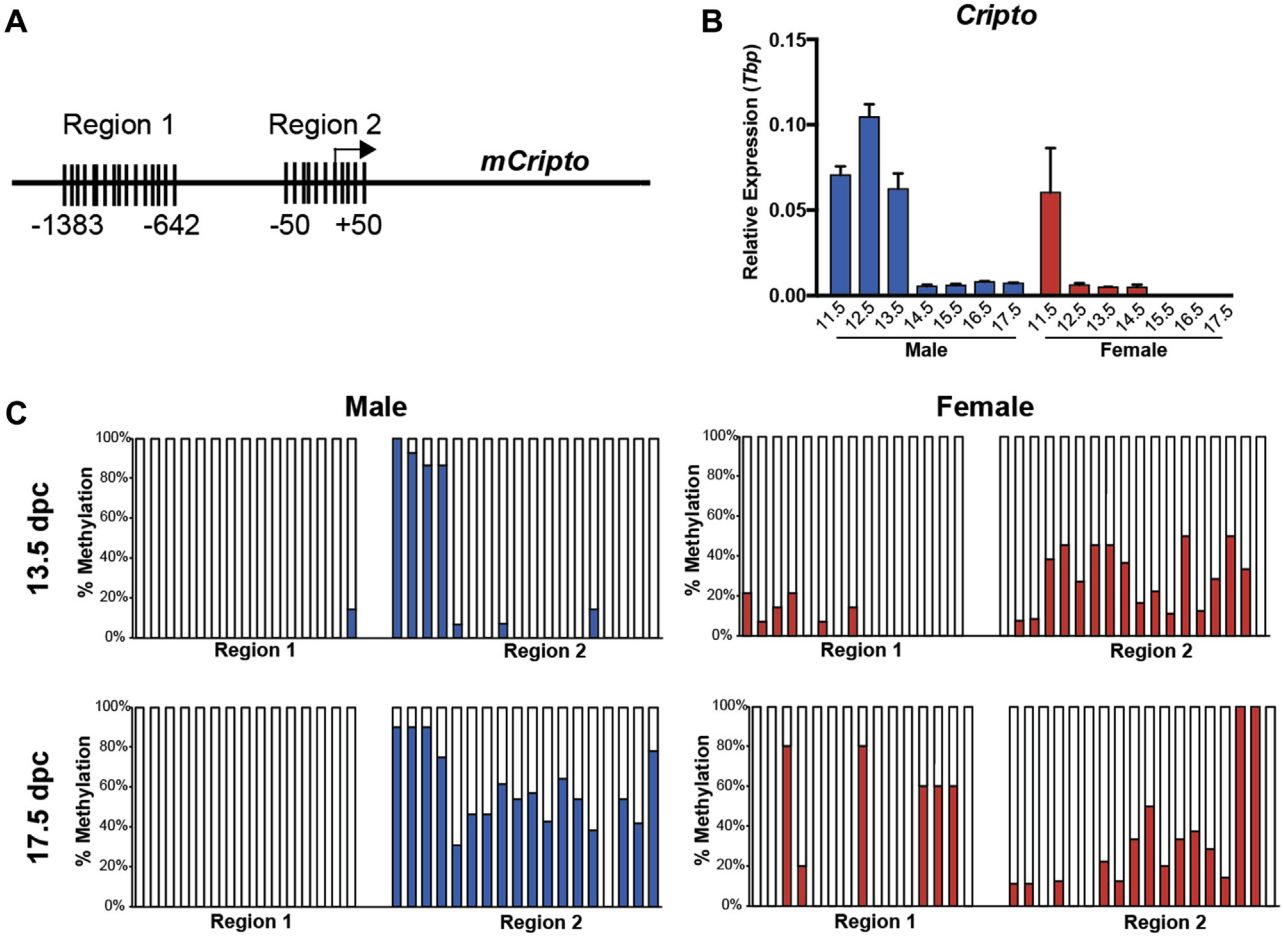

Figure 1 – Bisulfite analysis of CpG methylation in the promoter region of *Cripto* in 13.5 and 17.5 dpc germ cells. (A) The mouse *Cripto* promoter has two CpG islands in the proximal promoter region: Region 1 at position -1383 – 642 contains 15 CpG sites. Region 2 at position −50 – +50 contains 18 CpG sites. (B) *Cripto* is expressed maximally in male gonads at 12.5 dpc and has declined by 14.5 dpc. Expression is similar in male and female gonads at 11.5 dpc before becoming downregulated by 12.5 dpc in the female. qRT-PCR of pooled gonad-only male and female samples at 11.5–17.5 dpc. Expression normalized to *Tbp*; error bars represent ±S.E.M; $n = 3$. (C) Methylation (expressed as % methylation) for each CpG site are shown for purified male and female germ cells at 13.5 and 17.5 dpc. For each sample ≥10 clones were sequenced.

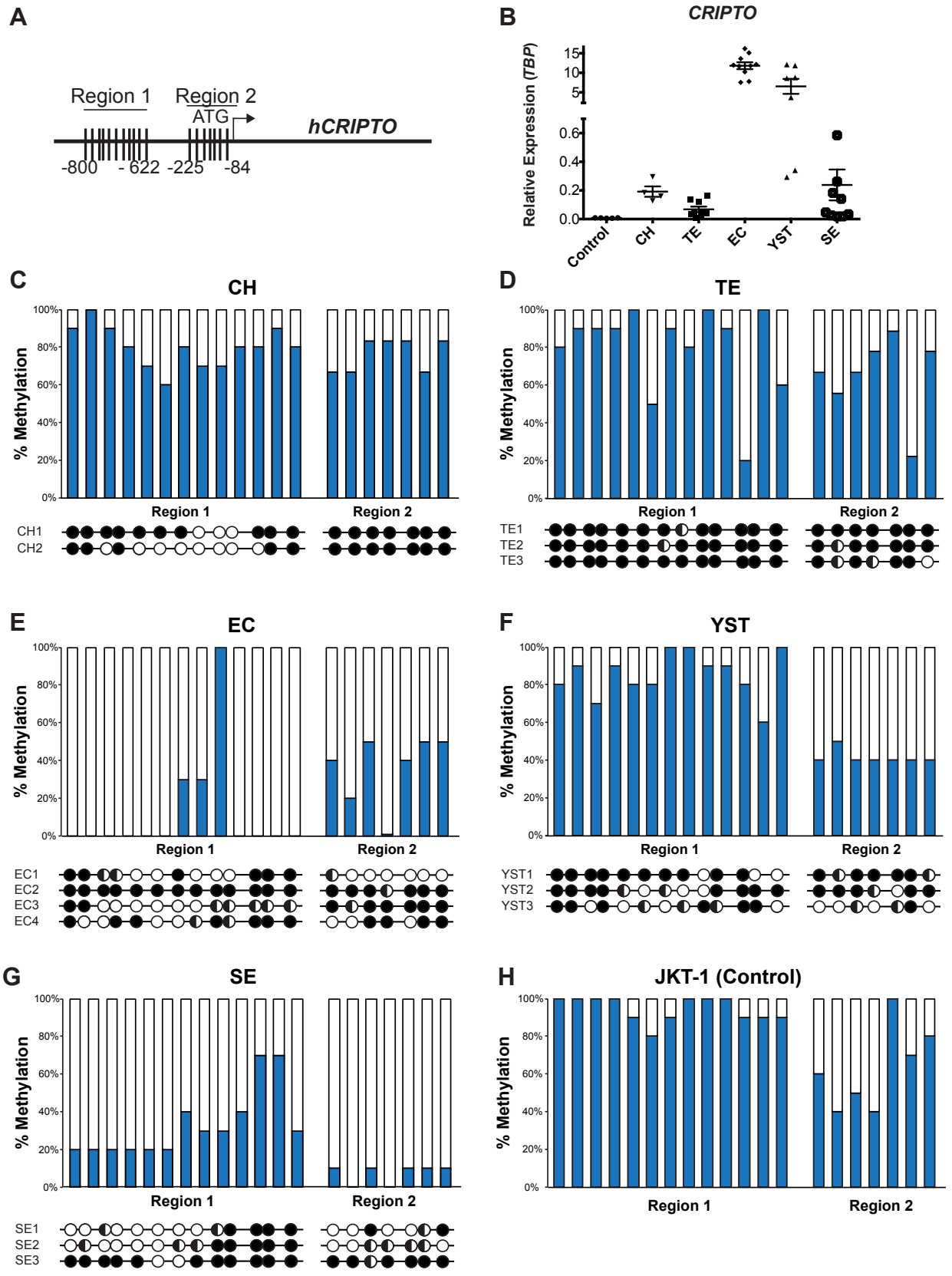

Figure 2 – Bisulfite analysis of GpG methylation in the promoter region of *CRIPTO* in GCC pathologies. (A) The human *CRIPTO* promoter has two CpG islands in the proximal promoter region: Region 1 at position −800 to −662 contains 13 CpG sites. Region 2 at position −225 to −84 contains 7 CpG sites. (B) qRT-PCR analysis of *CRIPTO* expression (Log2 scale) in normal testis (control) and NS and SE samples; $n = 5, 4, 9, 10,$

CRIPTO, promoter methylation was relatively low (24%; Figure 2G). These results were confirmed by direct sequencing (Figure 2C–G). As a negative control we included the JKT-1 cell line that is hypothesized to originate from a more mature germ cell (spermatocyte) (de Jong et al., 2007) and is negative for *CRIPTO* expression (Supplementary Figure 2A). In accordance with the lack of *CRIPTO* expression, JKT-1 cells were found to be highly methylated using colony sequencing (80%; Figure 2H). Together, these data indicate that hypermethylation of the Cripto promoter is associated with low gene expression in CH and TE and hypomethylation is associated with high gene expression in EC. This correlation does not hold true for SE and YST, which presumably utilize other methods (or methylated regions) for gene regulation.

We also included several GCC cell lines in the methylation analysis. *CRIPTO* was expressed most strongly at the mRNA level in the TERA-1 and NCCIT cells, at lower levels in NT2, TCam2 and 833 KE cells, and was undetectable in control JKT-1 cells (Supplementary Figure 2A). The EC (833 KE, NT2, NCCIT, TERA-1) and SE (TCam-2) cell lines, which express *CRIPTO* at varying levels, all showed low methylation by direct sequencing, although generally higher methylation in Region 2 compared to Region 1 (Supplementary Figure 2B).

Lastly, we performed *in vitro* demethylation of the genome by 5-azacytidine treatment of NT2 and TCam2 cell lines to observe the effect on *CRIPTO* expression. Although both cell lines display low levels of *CRIPTO* promoter methylation originally, upon 5-azacytadine treatment methylation was reduced even further in both regions, assessed by direct sequencing (Supplementary Figure 3A). Interestingly, qRT-PCR analysis revealed that *CRIPTO* mRNA expression was slightly reduced 48 h post treatment in both NT2 and TCam2 cells lines (0.5 and 0.2 fold, respectively; Supplementary Figure 3B). Because many genes have altered expression under such artificial conditions we also investigated expression of *NODAL* and the negative regulators of NODAL/CRIPTO signaling: *LEFTY1* and *LEFTY2* (Supplementary Figure 3B). We found *NODAL* expression to be greatly induced by demethylation in NT2 cells, and slightly reduced in TCam2 cells. Expression of both inhibitors *LEFTY1* and *LEFTY2* were induced robustly in both cell lines. We also assessed expression of pluripotency markers *SOX2*, *SOX17* and *GDF3* (Supplementary Figure 3B). Concordant with other studies, *SOX17* expression was not significantly altered under the demethylating conditions in either cell line (Wermann et al., 2010) and *SOX2* and *GDF3* were decreased in NT2 cells (Biswal et al., 2012). The DNA methyltransferase *DNMT3L*, was induced in both cell lines under these conditions, as also reported previously in TCam2 cells (Wermann et al., 2010). These results suggest that under the artificial condition of induced genome-wide demethylation, *CRIPTO* expression follows expression of other key pluripotency markers, consistent with its role in stem cell self-renewal and maintenance (Bianco et al., 2010; Biswal et al., 2012; Wei et al., 2005).

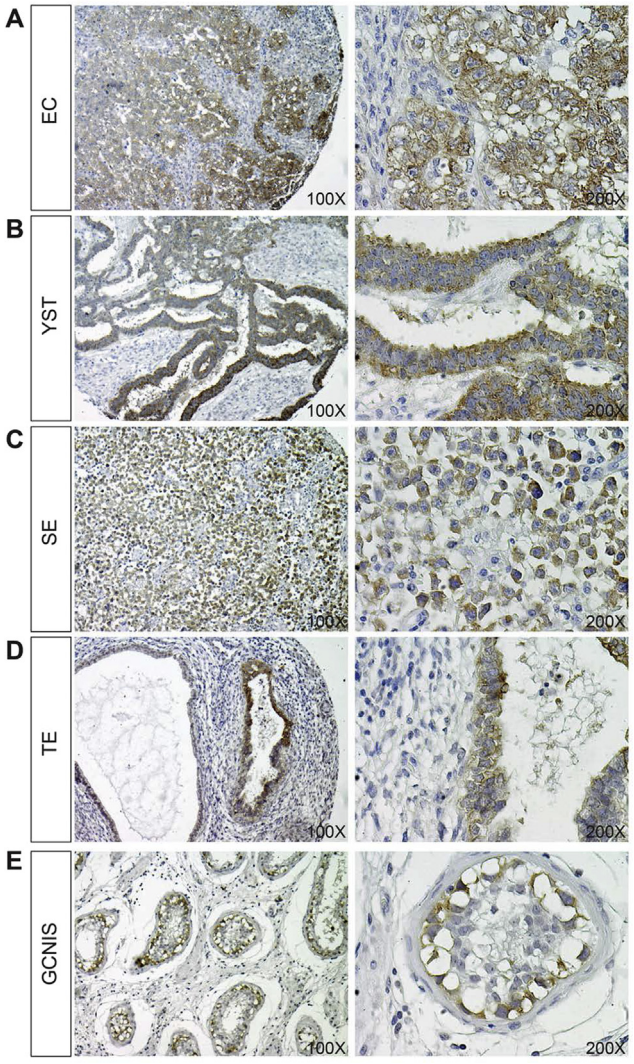

Figure 3 – Immunohistochemistry for CRIPTO expression (brown staining) in EC (A), YST (B), SE (C), TE (D) and GCNIS (E) pathologies, counterstained with haematoxylin. Images are representative of ≥8 biopsies analyzed for each subtype at a magnification of both 100 and 200× (left and right images, respectively).

3.3. *CRIPTO expression in GCNIS and GCC*

We next investigated CRIPTO protein expression in the same tissues and cell lines as investigated for methylation and mRNA expression. Based on qRT-PCR data (Figure 2A) we expected strong expression of CRIPTO in EC and YST, and low or no expression in SE and TE biopsies. We commissioned the production of a mouse monoclonal antibody raised

7, 10. Methylation for each CpG site is shown for CH (C), TE (D), EC (E), YST (F) SE (G) and JKT-1 control cell line (H). For each sample, graphs represent colony sequencing of ≥10 clones of one sample, each bar representing one CpG site (expressed at % methylation). Direct sequencing of 2–4 different tumor samples is presented as circles at each CpG site. Open circles represent unmethylated site, closed circles represent a methylated site and half-filled circles represent heterogeneity of methylation at this site within a given sample.

against part of the signal peptide of CRIPTO and verified that this antibody recognizes a single band in NT2 cells at the predicted molecular weight of 26 kDa (Supplementary Figure 4A). Further, this antibody outperformed the commercial R&D Systems capture antibody in recognizing recombinant CRIPTO in a sandwich ELISA assay (Supplementary Figure 4B). By immunohistochemistry we detected strong reactivity in EC and YST (Figure 3A,B). Despite a lower transcript abundance, we detected CRIPTO protein uniformly, but at lower intensity, in SE (lymphocytes were negative) (Figure 3C). In the differentiated GCC histology TE we found positive staining in small regions of differentiated cells, although large areas of tumor were negative for CRIPTO (Figure 3D).

We also investigated whether CRIPTO was expressed in GCNIS cells. Consistent with previous results showing elevated *CRIPTO* expression in testis biopsies containing GCNIS (Spiller et al., 2012), strong expression of membrane-bound CRIPTO was detected in GCNIS cells (verified by Pathologist J.W. Oosterhuis; Figure 3E). In normal testicular tissue, membranous CRIPTO was detectable only in spermatogonial stem cells (verified by J.W. Oosterhuis; Supplementary Figure 5A). Some positive staining was detected in nuclei of spermatocytes: we presume that this represents non-specific binding as is seen for various antibodies (unpublished observations). Spermatids and all interstitium were negative for CRIPTO. Negative controls omitting primary antibody showed no staining (Supplementary Figure 5B).

3.4. Soluble CRIPTO detection in GCC cell line media

Although GPI-anchored to the cell membrane, CRIPTO can be cleaved at this site and signal as a soluble ligand (Watanabe et al., 2007a, 2007b). The presence of soluble CRIPTO has been reported in the serum of patients with breast cancer, colon cancer and glioblastoma multiforme brain tumors (Bianco et al., 2006; Pilgaard et al., 2014) which suggests that it may be detectable, similarly, in serum of patients with GCC. Initially we investigated this possibility in GCC cell lines. By immunohistochemistry we found CRIPTO expressed in TCam2, TERA-1 and NT2 cell lines, but not JKT-1 control cells (Figure 4A). Although TERA-1 and NT2 cells uniformly expressed CRIPTO, individual TCam2 cells displayed variable expression (absent to strong). We next evaluated the concentration of CRIPTO present in the media of each of these cell lines using sandwich ELISA. CRIPTO was undetectable in JKT-1 culture media (Figure 4B), consistent with the negative immunohistochemistry and qRT-PCR data (Supplementary Figure 1A). Highest average levels of cleaved CRIPTO were detected in media of the EC cell lines NT2 (11.7 ng/ml) and TERA-1 (8.7 ng/ml), and lower levels in SE cell line TCam2 (1.4 ng/ml) (Figure 4B). Levels of expression varied depending on confluency of the cells (ranging 10–100%), which is reflected in the range of values detected.

3.5. Soluble CRIPTO detection in GCC patient serum

Having found CRIPTO detectable in GCC by immunohistochemistry (Figure 3) we next assessed serum of patients with various GCC pathologies (Figure 5 and Table 1). Using ELISA, only one of 15 control patients (6.6%) generated

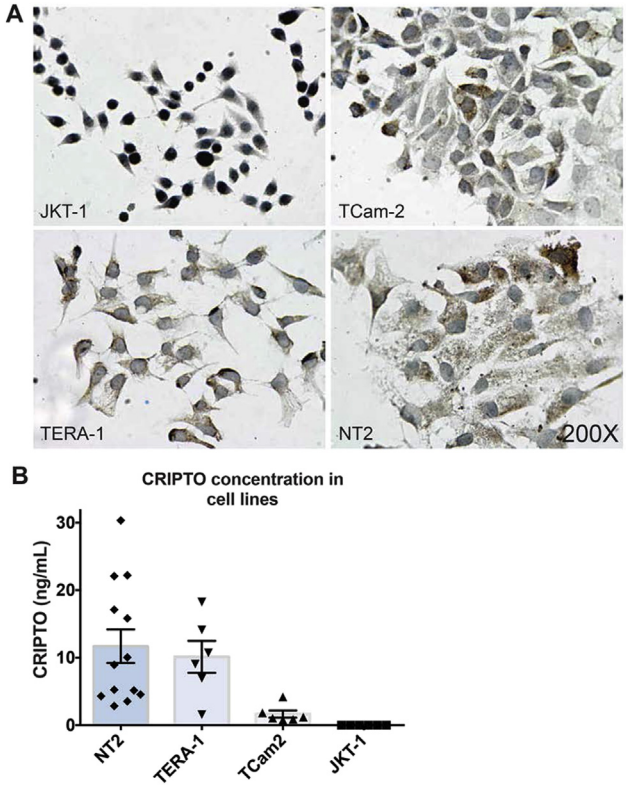

Figure 4 – (A) Immunohistochemistry for CRIPTO expression in JKT-1, TCam-2, TERA-1 and NT2 cell lines (B) CRIPTO concentration (ng/mL) assessed by ELISA in cell culture media collected from cell lines NT2 (range: 2.85–30.35), TERA-1 (range: 1.58–18.28), TCam2 (range: 0.78–4.19) and JKT-1 (range: 0.0–0.0) at varying confluences (ranging 10–100%). Error bars represent ±S.E.M; n = 13,6,6,6.

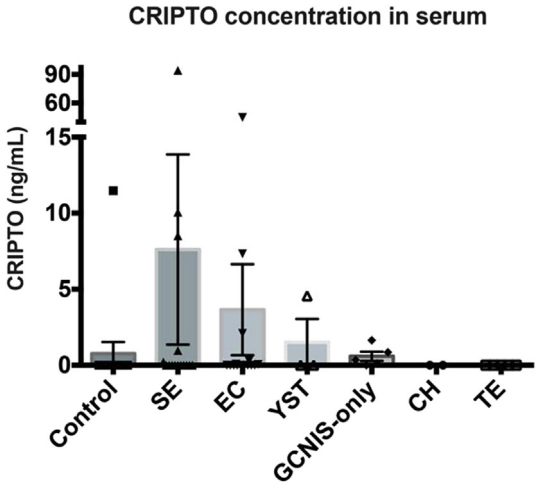

Figure 5 – CRIPTO concentration (ng/mL) assessed by ELISA in patient serum of control (no testicular malignancy), SE, EC, YST, GCNIS-only, CH and TE pathologies. Error bars represent ±S.E.M; n = 15,15,15,3,5,1,5.

Table 1 – CRIPTO concentration in serum.

Patient group	No. Positive samples/total	CRIPTO concentration (ng/mL)		Statistics	
		Mean (SD)	Range	P[a]	P[b]
Control	1/15	0.77 (2.97)	0.0–11.48	–	–
SE	5/15	7.61 (24.22)	0.0–94.36	0.1433	0.0437
EC	6/15	3.66 (11.59)	0.0–44.98	0.0695	0.0178
YST	1/3	1.52 (2.63)	0.0–4.56	0.3137	0.1875
GCNIS-only	4/5	0.59 (0.67)	0.0–1.63	0.0049	0.0016
TE	0/5	–	–	–	–
CH	0/1	–	–	–	–

a Mann–Whitney *U* test of patient group versus control.
b Mann–Whitney *U* test of patient group versus control excluding positive outlier.

detectable CRIPTO in serum (Control patients had no testicular malignancy at biopsy, but presented with some testicular abnormality such as testicular torsion or epididymitis. Inclusion in this 'control' group did not exclude the possibility that other somatic malignancies may have been present without our knowledge at the time of serum collection). Highest levels of CRIPTO were detected in SE samples, of which 5 of 15 (33%) were positive and had an average value of 7.6 ± 24.2 ng/ml. The large standard deviation in this group is accounted for by one sample, of unknown clinical stage, that generated an unusually high reading of 94.36 ng/ml of CRIPTO. In EC serum samples, CRIPTO was detected in 6 of 15 (33%) at an average concentration of 3.6 ± 11.6 ng/ml. One of 3 YST samples (33%) was positive (average 1.5 ± 2.6 ng/ml). Lower levels of CRIPTO were detected in 4 of the 5 GCNIS-only samples (80%). The GCNIS-only group had an average concentration of 0.6 ± 0.7 ng/ml and was distinct, in a statistically significant manner, from the control group. The 5 TE and 1 CH serum samples were negative for CRIPTO expression in this assay. When these data were analyzed against the control group omitting the outlying sample (high CRIPTO concentration of 11.5 ng/ml), we found that EC, SE and GCNIS-only groups were significantly distinct from control (Table 1).

4. Discussion

Previous studies in mice have established a role for Nodal/Cripto signaling in the maintenance of germ cell pluripotency during a short window of germ cell development (Spiller et al., 2012). This period of development is believed to correspond to a window of vulnerability for germ cell transformation into GCNIS, the common precursor of all GCC. The finding that CRIPTO is relatively highly expressed in GCC (Baldassarre et al., 2001; Spiller et al., 2012) suggests that embryonic CRIPTO expression may fail to extinguish during malignant transformation. In the present study we found that epigenetic factors may be responsible for this aberrant expression during adult life. We also provide proof-of-principle that detection of cleaved CRIPTO protein in serum might be a useful avenue for prognostic and/or diagnostic application to GCC.

As expected, we found that methylation was highest in mouse germ cell populations where *Cripto* expression is low. Of the two regions analyzed in fetal germ cells, it appears Region 2, spanning the transcription start site, is more important: CpG sites in Region 2 became hypermethylated in XY germ cells as expression declined, while the more distal CpG sites (Region 1) remained hypomethylated at both timepoints. There was little change to methylation in XX germ cells in either region over time, likely because they do not undergo genome-wide remethylation but, rather, enter meiosis (La Salle et al., 2004; McLaren, 2003; Western et al., 2010). We speculate that the hypomethylation of Region 1 is responsible for allowing the transient expression of *Cripto* in XY germ cells, and further, that hypermethylation of this site may be a meiosis-specific methylation pattern in XX germ cells that helps prevent expression of *Cripto* that might otherwise disrupt meiosis. Methylation analysis of sexed, 11.5 dpc germ cells before sex-specific gene expression begins, although technically challenging, would shed light on these possibilities.

Similarly to mouse, the human *CRIPTO* promoter has two regions enriched for CpG sites (Bianco et al., 2013; Watanabe et al., 2010). In our cell line analysis, we find both regions generally hypomethylated in SE and NS cell lines that express *CRIPTO*, regardless of relative expression levels, and both regions hypermethylated in the control cell line that is negative for *CRIPTO* expression. These results concur with recent findings using DNA methylation PCR for Region 2 of *CRIPTO* in which <10% of this promoter region was found to be methylated (Bianco et al., 2013). In order to link methylation of these regions to CRIPTO gene expression, Watanabe et al. (2010) performed retinoic acid-induced DNA methylation in the EC cell line NT2/D1 and showed that time-dependent methylation of the same CpG regions we investigated, correspond to reduction in CRIPTO expression. Further, they showed that differences in methylation of CpG Region 1 correspond to gene expression in this cell line, supporting the claim that methylation is partially responsible for CRIPTO gene regulation (Watanabe et al., 2010). Here we tested the opposite approach of *in vitro* genome wide demethylation using 5-azacytadine in NT2 and TCam2 cells and found that under these conditions CRIPTO expression was slightly decreased post-treatment. Although somewhat surprising, this could be due to a combination of factors, including that these regions are already sufficiently hypomethylated or that upregulation of negative inhibitors of CRIPTO/NODAL signaling such as LEFTY1, -2 (and many others that we did not test for) could have negative feedback on *CRIPTO* expression. In addition to these

possibilities it is also possible, and likely, that CRIPTO falls within the complement of classic 'pluripotency' factors that become downregulated under the artificial *in vitro* conditions of global demethylation (along with *NANOG*, *SOX2*, *GDF3* and MYC target genes; (Biswal et al., 2012)).

In the GCC samples, we found a clear correlation between *CRIPTO* promoter hypermethylation and low *CRIPTO* expression in TE and CH tumor subtypes, and *vice versa* for EC. These correlations were not found for YST and SE. Instead, in YST samples (which display high levels of *CRIPTO* expression), we found high levels of methylation in Region 1 of the *CRIPTO* promoter, while Region 2 showed moderate levels of methylation. However, as YST is known to display high levels of global methylation (Amatruda et al., 2013; Furukawa et al., 2009), it is possible that the moderate level of methylation in Region 2 is sufficient for gene transcription, although it is likely that additional mechanisms are involved. Similarly, for SE, the hypomethylation observed in our findings is seemingly contrary to low *CRIPTO* expression, but is consistent with the global hypomethylation that characterizes this GCC subtype (Netto et al., 2008; Smiraglia et al., 2002; Wermann et al., 2010). It is possible that modest methylation of Region 1 is sufficient to suppress gene transcription in this genomic environment of global hypomethylation.

Exactly how a GCNIS cell transforms into the two distinct tumor types, SE and NS, which are characterized by hypo- and hypermethylation, respectively, is unknown. This issue is of interest because of the different sensitivity of the SE and NS elements to irradiation and cisplatin-based chemotherapy. GCNIS cells, like SE, exhibit global hypomethylation, akin to their fetal germ cell precursors, so *de novo* methylation is thought to be largely responsible for establishment of the methylation profile in the overt tumor (Almstrup et al., 2010; Netto et al., 2008; Wermann et al., 2010). Based on our fetal germ cell data, we might expect *CRIPTO* Region 1 to be completely hypomethylated and Region 2 to have variable methylation in a given GCNIS cell. Indeed it has been shown that differing levels of CRIPTO expression and methylation in the NT2 human EC cell line correlate with malignancy potential of these cells (Watanabe et al., 2010). It will be interesting to investigate whether individual GCNIS cells express CRIPTO at varying levels, and whether methylation of Region 1 may be predictive of a GCNIS cell that will give rise to EC (hypomethylation) or SE (moderate levels of methylation).

We found in our cell line analysis that protein expression of CRIPTO, detected by immunohistochemistry, was comparable between NT2 and TERA-1 cells, despite lower gene expression in NT2 cells. This discrepancy is likely the result of different confluency of the cells when assayed for RNA and protein, as confluency was seen to greatly affect levels of soluble CRIPTO detected in media using the ELISA assay. This is consistent with a report from Watanabe et al. (2010) that see CRIPTO expression decline in NT2/D1 cells at confluency. Similarly, although we expected strong protein expression of CRIPTO in EC and YST, based on other reports and our own gene expression data, we were surprised to find that it could also be detected in SE and small regions of TE biopsies, where gene expression is overall low. However, expression of CRIPTO in GCNIS makes it extremely likely that it would also be expressed in SE, as these two cell types share similar expression profiles (Almstrup et al., 2005). We don't consider it likely that our antibody is detecting an unspecific target in SE based on the Western blot results and the fact that our immunohistochemistry data was corroborated by the independently-tested antibodies in the sandwich ELISA, which detected CRIPTO protein in the SE cell line TCam2 and in serum of patients with SE. This surprising finding of low gene expression with high protein detection is not unique, and for example has also reported for GDF3, in which the transcript is predominantly expressed in EC and YST but the protein is also detected in GCNIS and SE (Gopalan et al., 2009; Korkola et al., 2006). This similarity is of interest as GDF3 is a known ligand for CRIPTO and is one of the stem cell genes in the 200 kb region of chromosome 12p12.31 commonly over-represented in both SE and NS (Roelofs et al., 2000; Zafarana et al., 2003). The overlapping expression patterns of CRIPTO and GDF3 in GCNIS and the GCC subtypes (Figure 6) suggests that GDF3 (alone, or in combination with NODAL) could trigger CRIPTO activation. In this context it is of interest to mention that gain of 12p is

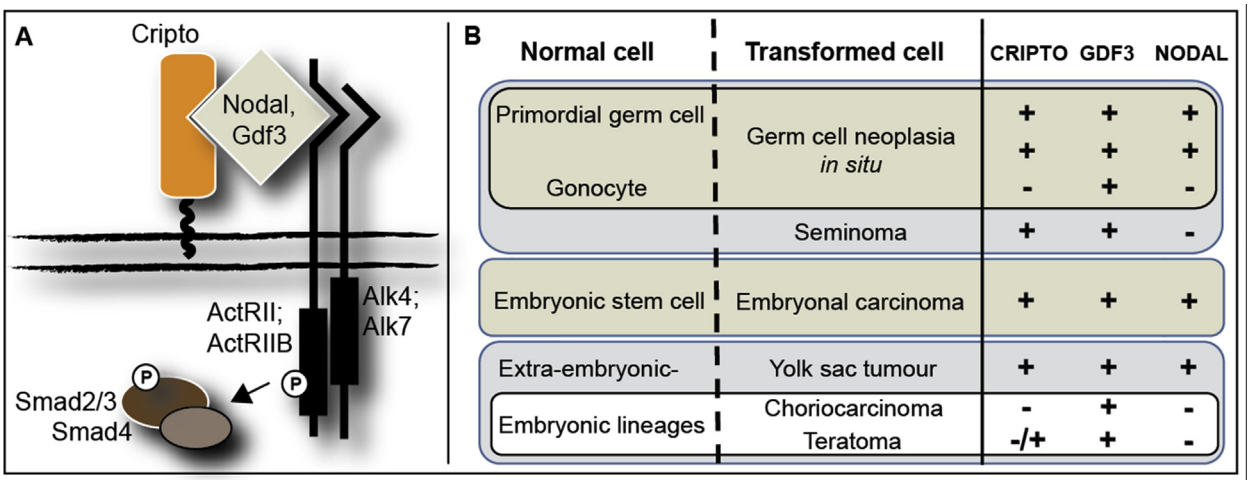

Figure 6 – Schematic of CRIPTO/NODAL/GDF3 signaling (A) and the combinations of receptor/ligand expression in normal germ cells, embryonic stem cells and the subtypes of GCC (B). Symbols represent positive expression (+), negative expression (−) and heterogeneous expression (−/+).

related to progression from GCNIS to either SE or NS (Rosenberg et al., 2000). It will be interesting to determine how the specific combinations of CRIPTO/GDF3/NODAL contribute to the malignancy potential of each subtype, a question that we are now investigating.

Screening using serum markers is minimally invasive, rapid and cost-effective. Detection of CRIPTO for diagnostic and prognostic purposes has been assessed for breast, colon and brain cancer (Bianco et al., 2006; Pilgaard et al., 2014); both studies similarly utilized sandwich ELISA for CRIPTO detection. In our analysis we detected highest average CRIPTO readings for SE followed by EC, YST then GCNIS-only samples, of which % sensitivity was 33%, 40%, 33%, 33% and 80% respectively. Our false positive rate was 6%, however it is possible that the presence of CRIPTO in this one sample is attributable to another undetected malignancy at the time of serum collection (CRIPTO is expressed in a wide range of epithelial cancers (Normanno et al., 2001)). A larger sample size would reduce the effect such outliers have on the data set. Our background reading of CRIPTO expression was 0 ng/ml for 14 of 15 control samples. Conversely, Bianco et al. (2006) detected CRIPTO levels in plasma of above 0.07 ng/ml for all samples ($n = 21$) and Pilgaard et al. (2014) above 0.3 ng/ml for all samples ($n = 27$). Discrepancies between our basal levels of CRIPTO and those from the previous studies can most likely be attributable to differences in the ELISA assays (Bianco et al., 2006) and serum dilution factor differences (Bianco et al., 2006; Pilgaard et al., 2014). We found a 1:2 dilution factor necessary to consistently achieve good linearity-of-dilution and spike-and-recovery efficiencies when optimizing our assay (data not shown). It may be possible to increase the sensitivity of our assay by increasing the capture and/or detection antibody concentrations.

An alternative and more promising approach that we are currently pursuing is detection of CRIPTO using ELISA in semen samples. As the CRIPTO-expressing GCNIS and GCC cells are in close proximity with semen, it is feasible that this will prove highly sensitive for our diagnostic and prognostic purposes. So far, CRIPTO is undetectable in 6/6 controls (malignancy-free, normozoospermic) in our assay optimized for semen (data not shown). A great advantage of this approach, in addition to a likely increase in sensitivity, is that positivity for CRIPTO in semen would presumably be a specific indicator of the precursor of GCC, unlike positivity in serum, as outlined above.

In conclusion, our studies have highlighted regions of the *CRIPTO* promoter that appear to be differentially methylated in fetal germ cells and GCC derived from incorrect germ cell differentiation. We have also demonstrated for the first time the potential suitability of CRIPTO as a serological marker for diagnostic and/or prognostic purposes for GCC. We are now investigating whether detection in semen may offer an alternative and potentially more sensitive means for GCC diagnosis.

Disclosure/conflicts of interest

No conflicts of interest are declared.

Acknowledgements

We thank Prof Sohei Kitazawa and Prof Riko Kitazawa from the Department of Molecular Pathology, Ehime University Graduate School of Medicine, Japan, for providing TCam2 cells. Flow cytometry was performed with the assistance of the Queensland Brain Institute Flow Cytometry Facility. This work was supported by the National Health and Medical Research Council [APP1030146] and Cancer Council Queensland [APP1012325]. CS is a University of Queensland Postdoctoral Fellow. PK is an NHMRC Senior Principal Research Fellow.

Appendix A. Supplementary data

Supplementary data related to this article can be found at http://dx.doi.org/10.1016/j.molonc.2015.11.003.

REFERENCES

Adami, H.O., Bergstrom, R., Mohner, M., Zatonski, W., Storm, H., Ekbom, A., Tretli, S., Teppo, L., Ziegler, H., Rahu, M., et al., 1994. Testicular cancer in nine northern European countries. Int. J. Cancer 59, 33–38.

Almstrup, K., Hoei-Hansen, C.E., Nielsen, J.E., Wirkner, U., Ansorge, W., Skakkebaek, N.E., Rajpert-De Meyts, E., Leffers, H., 2005. Genome-wide gene expression profiling of testicular carcinoma in situ progression into overt tumours. Br. J. Cancer 92, 1934–1941.

Almstrup, K., Nielsen, J.E., Mlynarska, O., Jansen, M.T., Jorgensen, A., Skakkebaek, N.E., Rajpert-De Meyts, E., 2010. Carcinoma in situ testis displays permissive chromatin modifications similar to immature foetal germ cells. Br. J. Cancer 103, 1269–1276.

Amatruda, J.F., Ross, J.A., Christensen, B., Fustino, N.J., Chen, K.S., Hooten, A.J., Nelson, H., Kuriger, J.K., Rakheja, D., Frazier, A.L., Poynter, J.N., 2013. DNA methylation analysis reveals distinct methylation signatures in pediatric germ cell tumors. BMC Cancer 13, 313.

Baldassarre, G., Tucci, M., Lembo, G., Pacifico, F.M., Dono, R., Lago, C.T., Barra, A., Bianco, C., Viglietto, G., Salomon, D., Persico, M.G., 2001. A truncated form of teratocarcinoma-derived growth factor-1 (cripto-1) mRNA expressed in human colon carcinoma cell lines and tumors. Tumour Biol. 22, 286–293.

Bianco, C., Castro, N.P., Baraty, C., Rollman, K., Held, N., Rangel, M.C., Karasawa, H., Gonzales, M., Strizzi, L., Salomon, D.S., 2013. Regulation of human Cripto-1 expression by nuclear receptors and DNA promoter methylation in human embryonal and breast cancer cells. J. Cell Physiol. 228, 1174–1188.

Bianco, C., Rangel, M.C., Castro, N.P., Nagaoka, T., Rollman, K., Gonzales, M., Salomon, D.S., 2010. Role of Cripto-1 in stem cell maintenance and malignant progression. Am. J. Pathol. 177, 532–540.

Bianco, C., Strizzi, L., Mancino, M., Rehman, A., Hamada, S., Watanabe, K., De Luca, A., Jones, B., Balogh, G., Russo, J., Mailo, D., Palaia, R., D'Aiuto, G., Botti, G., Perrone, F., Salomon, D.S., Normanno, N., 2006. Identification of cripto-1 as a novel serologic marker for breast and colon cancer. Clin. Cancer Res. 12, 5158–5164.

Biswal, B.K., Beyrouthy, M.J., Hever-Jardine, M.P., Armstrong, D., Tomlinson, C.R., Christensen, B.C., Marsit, C.J., Spinella, M.J., 2012. Acute hypersensitivity of pluripotent testicular cancer-derived embryonal carcinoma to low-dose 5-aza deoxycytidine is associated with global DNA damage-associated p53 activation, anti-pluripotency and DNA demethylation. PLoS One 7, e53003.

de Jong, J., Stoop, H., Gillis, A.J., van Gurp, R.J., van Drunen, E., Beverloo, H.B., Lau, Y.F., Schneider, D.T., Sherlock, J.K., Baeten, J., Hatakeyama, S., Ohyama, C., Oosterhuis, J.W., Looijenga, L.H., 2007. JKT-1 is not a human seminoma cell line. Int. J. Androl. 30, 350–365.

Furukawa, S., Haruta, M., Arai, Y., Honda, S., Ohshima, J., Sugawara, W., Kageyama, Y., Higashi, Y., Nishida, K., Tsunematsu, Y., Nakadate, H., Ishii, M., Kaneko, Y., 2009. Yolk sac tumor but not seminoma or teratoma is associated with abnormal epigenetic reprogramming pathway and shows frequent hypermethylation of various tumor suppressor genes. Cancer Sci. 100, 698–708.

Gopalan, A., Dhall, D., Olgac, S., Fine, S.W., Korkola, J.E., Houldsworth, J., Chaganti, R.S., Bosl, G.J., Reuter, V.E., Tickoo, S.K., 2009. Testicular mixed germ cell tumors: a morphological and immunohistochemical study using stem cell markers, OCT3/4, SOX2 and GDF3, with emphasis on morphologically difficult-to-classify areas. Mod. Pathol. 22, 1066–1074.

Klauzinska, M., Castro, N.P., Rangel, M.C., Spike, B.T., Gray, P.C., Bertolette, D., Cuttitta, F., Salomon, D., 2014. The multifaceted role of the embryonic gene Cripto-1 in cancer, stem cells and epithelial-mesenchymal transition. Semin. Cancer Biol. 29, 51–58.

Korkola, J.E., Houldsworth, J., Chadalavada, R.S., Olshen, A.B., Dobrzynski, D., Reuter, V.E., Bosl, G.J., Chaganti, R.S., 2006. Down-regulation of stem cell genes, including those in a 200-kb gene cluster at 12p13.31, is associated with in vivo differentiation of human male germ cell tumors. Cancer Res. 66, 820–827.

La Salle, S., Mertineit, C., Taketo, T., Moens, P.B., Bestor, T.H., Trasler, J.M., 2004. Windows for sex-specific methylation marked by DNA methyltransferase expression profiles in mouse germ cells. Dev. Biol. 268, 403–415.

Looijenga, L.H., de Leeuw, H., van Oorschot, M., van Gurp, R.J., Stoop, H., Gillis, A.J., de Gouveia Brazao, C.A., Weber, R.F., Kirkels, W.J., van Dijk, T., von Lindern, M., Valk, P., Lajos, G., Olah, E., Nesland, J.M., Fossa, S.D., Oosterhuis, J.W., 2003. Stem cell factor receptor (c-KIT) codon 816 mutations predict development of bilateral testicular germ-cell tumors. Cancer Res. 63, 7674–7678.

McFarlane, L., Truong, V., Palmer, J.S., Wilhelm, D., 2013. Novel PCR assay for determining the genetic sex of mice. Sex Dev. 7, 207–211.

McLaren, A., 2003. Primordial germ cells in the mouse. Dev. Biol. 262, 1–15.

Mosselman, S., Looijenga, L.H., Gillis, A.J., van Rooijen, M.A., Kraft, H.J., van Zoelen, E.J., Oosterhuis, J.W., 1996. Aberrant platelet-derived growth factor alpha-receptor transcript as a diagnostic marker for early human germ cell tumors of the adult testis. Proc. Natl. Acad. Sci. U. S. A 93, 2884–2888.

Netto, G.J., Nakai, Y., Nakayama, M., Jadallah, S., Toubaji, A., Nonomura, N., Albadine, R., Hicks, J.L., Epstein, J.I., Yegnasubramanian, S., Nelson, W.G., De Marzo, A.M., 2008. Global DNA hypomethylation in intratubular germ cell neoplasia and seminoma, but not in nonseminomatous male germ cell tumors. Mod. Pathol. 21, 1337–1344.

Normanno, N., Bianco, C., De Luca, A., Salomon, D.S., 2001. The role of EGF-related peptides in tumor growth. Front Biosci. 6, D685–D707.

Oosterhuis, J.W., Looijenga, L.H., 2005. Testicular germ-cell tumours in a broader perspective. Nat. Rev. Cancer 5, 210–222.

Pilgaard, L., Mortensen, J.H., Henriksen, M., Olesen, P., Sorensen, P., Laursen, R., Vyberg, M., Agger, R., Zachar, V., Moos, T., Duroux, M., 2014. Cripto-1 expression in glioblastoma multiforme. Brain Pathol. 24, 360–370.

Roelofs, H., Mostert, M.C., Pompe, K., Zafarana, G., van Oorschot, M., van Gurp, R.J., Gillis, A.J., Stoop, H., Beverloo, B., Oosterhuis, J.W., Bokemeyer, C., Looijenga, L.H., 2000. Restricted 12p amplification and RAS mutation in human germ cell tumors of the adult testis. Am. J. Pathol. 157, 1155–1166.

Rosenberg, C., Van Gurp, R.J., Geelen, E., Oosterhuis, J.W., Looijenga, L.H., 2000. Overrepresentation of the short arm of chromosome 12 is related to invasive growth of human testicular seminomas and nonseminomas. Oncogene 19, 5858–5862.

Shen, M.M., 2007. Nodal signaling: developmental roles and regulation. Development 134, 1023–1034.

Skakkebaek, N.E., Berthelsen, J.G., Giwercman, A., Muller, J., 1987. Carcinoma-in-situ of the testis: possible origin from gonocytes and precursor of all types of germ cell tumours except spermatocytoma. Int. J. Androl. 10, 19–28.

Smiraglia, D.J., Szymanska, J., Kraggerud, S.M., Lothe, R.A., Peltomaki, P., Plass, C., 2002. Distinct epigenetic phenotypes in seminomatous and nonseminomatous testicular germ cell tumors. Oncogene 21, 3909–3916.

Sonne, S.B., Almstrup, K., Dalgaard, M., Juncker, A.S., Edsgard, D., Ruban, L., Harrison, N.J., Schwager, C., Abdollahi, A., Huber, P.E., Brunak, S., Gjerdrum, L.M., Moore, H.D., Andrews, P.W., Skakkebaek, N.E., Rajpert-De Meyts, E., Leffers, H., 2009. Analysis of gene expression profiles of microdissected cell populations indicates that testicular carcinoma in situ is an arrested gonocyte. Cancer Res. 69, 5241–5250.

Spiller, C.M., Bowles, J., Koopman, P., 2013. Nodal/Cripto signaling in fetal male germ cell development: implications for testicular germ cell tumors. Int. J. Dev. Biol. 57, 211–219.

Spiller, C.M., Feng, C.W., Jackson, A., Gillis, A.J., Rolland, A.D., Looijenga, L.H., Koopman, P., Bowles, J., 2012. Endogenous Nodal signaling regulates germ cell potency during mammalian testis development. Development 139, 4123–4132.

Szabo, P.E., Hubner, K., Scholer, H., Mann, J.R., 2002. Allele-specific expression of imprinted genes in mouse migratory primordial germ cells. Mech. Dev. 115, 157–160.

van de Geijn, G.J., Hersmus, R., Looijenga, L.H., 2009. Recent developments in testicular germ cell tumor research. Birth Defects Res. C Embryo Today 87, 96–113.

Watanabe, K., Bianco, C., Strizzi, L., Hamada, S., Mancino, M., Bailly, V., Mo, W., Wen, D., Miatkowski, K., Gonzales, M., Sanicola, M., Seno, M., Salomon, D.S., 2007a. Growth factor induction of Cripto-1 shedding by glycosylphosphatidylinositol-phospholipase D and enhancement of endothelial cell migration. J. Biol. Chem. 282, 31643–31655.

Watanabe, K., Hamada, S., Bianco, C., Mancino, M., Nagaoka, T., Gonzales, M., Bailly, V., Strizzi, L., Salomon, D.S., 2007b. Requirement of glycosylphosphatidylinositol anchor of Cripto-1 for trans activity as a Nodal co-receptor. J. Biol. Chem. 282, 35772–35786.

Watanabe, K., Meyer, M.J., Strizzi, L., Lee, J.M., Gonzales, M., Bianco, C., Nagaoka, T., Farid, S.S., Margaryan, N., Hendrix, M.J., Vonderhaar, B.K., Salomon, D.S., 2010. Cripto-1 is a cell surface marker for a tumorigenic, undifferentiated subpopulation in human embryonal carcinoma cells. Stem Cells 28, 1303–1314.

Wei, C.L., Miura, T., Robson, P., Lim, S.K., Xu, X.Q., Lee, M.Y., Gupta, S., Stanton, L., Luo, Y., Schmitt, J., Thies, S., Wang, W., Khrebtukova, I., Zhou, D., Liu, E.T., Ruan, Y.J., Rao, M., Lim, B., 2005. Transcriptome profiling of human and murine ESCs identifies divergent paths required to maintain the stem cell state. Stem Cells 23, 166–185.

Wermann, H., Stoop, H., Gillis, A.J., Honecker, F., van Gurp, R.J., Ammerpohl, O., Richter, J., Oosterhuis, J.W., Bokemeyer, C., Looijenga, L.H., 2010. Global DNA methylation in fetal human germ cells and germ cell tumours: association with differentiation and cisplatin resistance. J. Pathol. 221, 433–442.

Western, P.S., van den Bergen, J.A., Miles, D.C., Sinclair, A.H., 2010. Male fetal germ cell differentiation involves complex repression of the regulatory network controlling pluripotency. FASEB J. 24, 3026–3035.

Zafarana, G., Grygalewicz, B., Gillis, A.J., Vissers, L.E., van de Vliet, W., van Gurp, R.J., Stoop, H., Debiec-Rychter, M., Oosterhuis, J.W., van Kessel, A.G., Schoenmakers, E.F., Looijenga, L.H., Veltman, J.A., 2003. 12p-amplicon structure analysis in testicular germ cell tumors of adolescents and adults by array CGH. Oncogene 22, 7695–7701.